Sheng, X., Clay, D.C. and Allport, John

Dynamics of mistuned radial turbine wheels

DYNAMICS OF MISTUNED RADIAL TURBINE WHEELS

X Sheng, DC Clay and J Allport
Holset Engineering Co Ltd, St Andrew's Road, Huddersfield, HD1 6RA, England

This paper presents investigations carried out at Holset into the dynamics of mistuned radial turbine wheels, including a literature review, a lumped parameter model, identification of the most responsive blade, distribution of the peak maximum order response and a method of mistuning identification.

INTRODUCTION AND A LITERATURE REVIEW

Mistuning in bladed wheels is the phenomenon of random and unavoidable blade-to-blade variations in geometry and material due to the casting process of the wheels. A mistuned wheel may exhibit vibration localisation and amplification, in which few blades have responses much greater than those of other blades and the tuned response. These mistuning effects not only significantly reduce the high cycle fatigue (HCF) life of the wheel, but also make it difficult to predict and measure the representative response.

Mistuning has been studied for over 30 years. Mistuning may be investigated from a statistical point of view due to its random nature. In stochastic structural dynamics, efforts have been made to use the perturbation method to establish analytical relationships between probability density functions of random parameters in a structural dynamic system and those of the required outputs (*e.g.* natural frequencies and forced responses) [1, 2]. Perturbation method requires no natural frequency of the unperturbed (tuned) system is repeated. This is not the case for a tuned bladed wheel. An alternative to this approach is to derive a much reduced (compared to a conventional finite element) model of high computational efficiency with part of the model parameters being random variables. The distributions of the random parameters are estimated from measurement and statistical results are produced from the reduced model by performing a large number of calculations. Different techniques have been developed to produce a reduced model. Refs [3, 4 and 5] represent a mistuned system using a lumped parameter model consisting of masses and springs. Such a model has a high computational efficiency but is difficult to capture vibration of high modes. Refs [6, 7 and 8] model a mistuned system using the component mode synthesis technique in which the first few modes, which are produced using FEM, of each component (substructure) of the system are employed to approximate vibration of the whole system. In addition to the sub-structural modes of a mistuned system, modes of the corresponding tuned system have also been used to synthesise the vibration of the mistuned system [9]. Other efficient modelling approaches are also attempted [10, 11].

Though statistics may be performed using a reduced model, mistuning identification for individual mistuned wheels is still desirable. Mistuning is identified normally from some, often inadequate, measured data, leaving the problem indeterminate. To obtain a set of unique parameters, extra conditions must be assumed. Two mistuning identification methods are suggested in Refs [12] and [13] in which blades are represented by multi-mass-spring systems coupled with each other and the hub (disk) is rigid and fixed. The first, termed *the random modal stiffness approach* (RMS), assumes mistuning exists in the stiffness matrices of the blades only and the mistuned modal shapes are not significantly different from the tuned ones. Under such conditions, the mistuned stiffness matrix of a blade can be determined straightforwardly by measuring *all* the mistuned blade frequencies (not the bladed disk system frequencies). The second is termed *the maximum likelihood approach* (ML). In this approach, both the mass and stiffness matrices of a blade are allowed to be mistuned. By assuming a joint probability density function for the stiffness and mass matrices, the mistuned mass and stiffness matrices are estimated under the condition that they give the measured blade frequencies while at the same time make the probability density function maximum. It is illustrated that the ML approach works better than the RMS approach in terms of the mean and standard deviation of the maximum forced vibration of the blades subject to order excitations. The difficulty in using the ML approach is how to choose correctly the type of the joint PDF and its parameters. It is also the fact that this method is based on the blade alone frequencies which may not be measurable for turbocharger turbine wheels since the blades cannot be removed from the hub.

Another mistuning identification method, presented in Refs [14] and [15], is based on the *fundamental mistuning model* developed in Ref [11]. There are four assumptions in the fundamental mistuning model: a) only a single, isolated family of modes will be excited; b) the strain energy of that family's modes is primarily in the blades; c) the family's natural frequencies are closely spaced; and finally d) mistuning is small. There is another assumption in the model which has not been stated explicitly: modes in this family can be approximated by a weighted sum of a number of tuned modes. To identify mistuning, the mistuned frequencies and modal shapes of that family must be measured. Once the mistuning is determined, the model can be used to predict responses to order excitations which mainly excite that family of modes. In other words, the excitation frequency must be close to the average of the frequencies of that family of modes. The challenge of using this method lies in accurate measurement of the mistuned modal shapes. This is true because the natural frequencies are closely spaced.

Mistuning effects such as vibration localisation and amplification are demonstrated in some of the aforementioned Refs [*e.g.* 8] using the developed model. It is found that mistuning effects are particularly prominent near the so-called veering of the corresponding tuned system. Though the veering phenomenon is to be explained, the vibration localisation phenomenon is interpreted in a review paper [16] using the stability theory. It is numerically demonstrated in Ref [17] that intentional mistuning may be used to depress some of the negative effects of the random mistuning. Though effort is made in [17] to explore the mechanism of intentional mistuning, a satisfactory explanation has not yet been achieved. A possible route to this may be the use of singular value decomposition, as shown in Ref [18].

It should be realised that previous research is mainly concerned with aero engine turbofans and only a little is on small radial flow turbines such as those in Holset turbochargers. Small radial flow turbines exhibit different dynamic behaviour from large aero turbofans and the effect of mistuning on the former is expected to be also different. It is also the fact that previous research has not considered the effect of centrifugal and Goliolis forces generated from the wheel rotation.

A SIMPLE MODEL FOR RADIAL TURBINE WHEELS

FE modal analysis

For a cyclically symmetric structure consisting of N identical sectors, vibration modes can be grouped by the nodal-diameter (ND) number n, where $n = 0, 1, 2, \cdots N/2$ if N is even or $n = 0, 1, 2, \cdots (N-1)/2$ if N is odd. In terms of a cylindrical coordinate system, the mode shapes, $\mathbf{u}^r$ and $\mathbf{u}^{r+1}$, of the rth and $(r+1)$th sectors are related by

$\mathbf{u}^{r+1} = e^{in2\pi/N}\mathbf{u}^{r}$ for the n-ND modes [19], where $i = \sqrt{-1}$. This shows a travelling wave pattern which extends to all the sectors. A natural frequency associating with a nodal-diameter number different from zero and $N/2$ (where N is even) repeats itself. Mistuning in general invalidates these modal properties.

To assist the development of a simple, lumped parameter model so that some investigations can be performed, natural frequencies and modal shapes are calculated using Ansys Workbench for a 12-blade turbine wheel (Fig 1). In the calculation the shaft is cut off from the weld boss and the weld boss is constrained in the axial direction. The calculated natural frequencies at 21°C are listed in Table 1 excluding the three zero-frequencies of rigid modes. The first two modes are 1-ND modes in which the hub rocks about a weld boss diameter. The frequencies of these two modes are denoted by $f_{T1} = \omega_{T1}/2\pi$. Frequencies of the third to eleventh modes correspond to nodal-diameter numbers from 2 to 6. They are close to each other (within 10 Hz, as the FE mesh gets finer, the discrepancies between these frequencies becomes smaller). These frequencies associate with modes in which the blades vibrate almost independently of each other and the hub stays motionless. This suggests that in these modes couplings between blades are weak and negligible. The average of these frequencies may be taken to be the first (cantilevered) blade frequency, denoted by $f_B = \omega_B/2\pi$. The twelfth mode, its frequency denoted by $f_R = \omega_R/2\pi$, is the first 0-ND mode in which the hub rotates like a rigid body and the blades vibrate in-phase and at the same amplitude. The next two modes are still 1-ND modes and the frequencies are denoted by $f_{T2} = \omega_{T2}/2\pi$. Further higher modes (e.g. the 15th and 16th modes in the table) have much higher frequencies and are not interested in this study.

Table 1 Natural frequencies of a 12-blade turbine wheel

Modes	Frequency (Hz)	Modes	Frequency (Hz)
1 (1-ND)	5725	9	6430
2 (1-ND)	5725	10	6430
3	6423	11	6433
4	6423	12 (0-ND)	6748
5	6425	13 (1-ND)	6940
6	6425	14 (1-ND)	6940
7	6427	15	11510
8	6427	16	11510

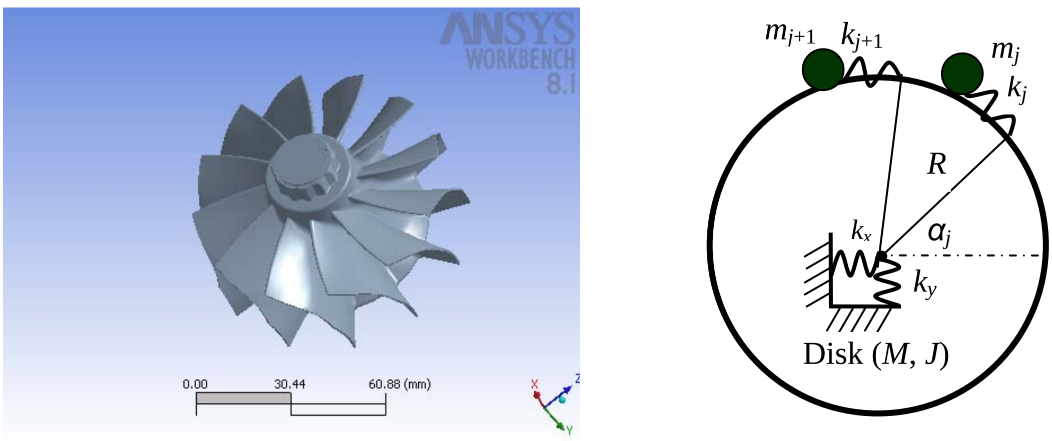

Figure 1 A turbine wheel and its lumped parameter model

A lumped parameter model

The FE calculation suggests that, for excitation at frequencies around or less than the blade frequency the wheel may be modelled as a rigid disk connecting a number of point masses through springs, as shown in Figure 1. The *j*th blade is represented by mass, m_j, connected to the disk by a spring of stiffness k_j, where $j = 1, 2, \cdots N$. The position connecting the spring at the disk is described by the radius *R* and angle α_j measured from the *x*-axis. The disk is described by mass *M* and inertial moment *J*. The disk is subject to stiffness, k_x and k_y, which model the rocking stiffness of the hub, and torsional stiffness, k_θ, from the shaft. Blade masses are restrained to vibrate in directions tangential to the disk periphery, so that the model has *N* + 3 degrees of freedom. The displacement of m_j relative to the disk is denoted by x_j. Displacement relative to the hub is used since it is proportional to the strain/stress in the blade. The displacements of the mass centre of the disk in the *x*- and *y*-directions are denoted by *x* and *y* and the vibrational rotation angle of the disk by θ. Without considering the spinning of the wheel, the differential equation of the model can be written as

$$\mathbf{M}\ddot{\mathbf{q}} + \mathbf{K}\mathbf{q} = \mathbf{Q} \tag{1}$$

where,

$$\mathbf{q} = (x, y, \theta, x_1, x_2, \cdots, x_N)^T \tag{2}$$

$\mathbf{Q}$ denotes the generalised force vector, $\mathbf{M} = (m_{ij})_{i,j=1,2,\cdots N+3}$ and $\mathbf{K} = (k_{ij})_{i,j=1,2,\cdots N+3}$ are mass and stiffness matrices with none-zero elements given by,

$$m_{11} = m_{22} = M + \sum_{j=1}^{N} m_j\ , \quad m_{33} = J + R^2 \sum_{j=1}^{N} m_j \tag{3a}$$

$$m_{13} = -R\sum_{j=1}^{N} m_j \sin\alpha_j\ , \quad m_{23} = R\sum_{j=1}^{N} m_j \cos\alpha_j \tag{3b}$$

$$m_{jj} = m_{j-3}, \quad m_{1j} = -m_{j-3}\sin\alpha_{j-3}, \quad m_{2j} = m_{j-3}\cos\alpha_{j-3}, \quad m_{3j} = Rm_{j-3} \tag{3c}$$

$$k_{jj} = k_{j-3},\ k_{11} = k_x,\ k_{22} = k_y,\ k_{33} = k_\theta \tag{3d}$$

where $j = 4, 5, \cdots, N+3$.

For the *n*th order excitation at frequency ω and of unit amplitude, the *j*th blade mass is subject to a force defined by $e^{in\alpha_j}e^{i\omega t}$. Thus in equation (1), $\mathbf{Q} = \tilde{\mathbf{Q}}e^{i\omega t}$, and

$$\tilde{\mathbf{Q}} = \left(-\sum_{j=1}^{N} e^{in\alpha_j}\sin\alpha_j, \sum_{j=1}^{N} e^{in\alpha_j}\cos\alpha_j, R\sum_{j=1}^{N} e^{in\alpha_j}, e^{in\alpha_1}, e^{in\alpha_2}, \cdots e^{in\alpha_N} \right)^T \tag{4}$$

Determination of model parameters for a tuned wheel

For the model shown in Fig 1 to be equivalent to a real bladed disk, the model parameters must be determined correctly. The blades may to assumed to be uniformly spaced, therefore α_j is given by

$$\alpha_j = (j-1)\frac{2\pi}{N} \quad (j = 1, 2, \cdots N) \tag{5}$$

The torsional stiffness of the shaft, k_θ, may be estimated from the shaft dimensions and material properties. For a tuned wheel in which the blades are identical to each other, there are only six parameters to be determined, which are M, J, R, $k_x = k_y$, $k_1 = k_j$ and $m_1 = m_j$ $(j = 2,3\cdots N)$.

To determine them, natural frequencies of the 0-ND and 1-ND modes of the lumped parameter model and the blade frequency are derived. They must be equal to the counterparts from the FE model and this gives four conditions for parameter determination. Now at each blade mass, a unit harmonic force at frequency ω is applied in the tangential direction. The displacement amplitude of the blade mass, observed from the ground, can be derived. A forced vibration FE analysis is performed under the same loading condition, *i.e.* a unit harmonic force at frequency ω is applied at each blade tip in the direction normal to the blade surface. From the analysis the normal displacement amplitude, A_1, of the blade tip can be worked out. The displacement amplitudes from the two models are equalised to provide the fifth condition. Finally a torque of unit amplitude and frequency ω is applied at the disk and the displacement amplitude of the blade mass observed from the ground is derived. This amplitude must be equal to the blade tip normal displacement amplitude, A_2 of the FE model under the same excitation, so that the sixth condition is produced. From these six conditions it can be shown

$$m_1 = \frac{\omega^2-\omega_R^2+\omega_B^2}{A_1\omega^2(\omega_R^2-\omega^2)}, \quad R = -\frac{A_1(\omega_R^2-\omega_B^2)}{NA_2(\omega^2-\omega_R^2+\omega_B^2)}, \quad J = \frac{Nm_1R^2\omega_B^2}{\omega_R^2-\omega_B^2}, \quad k_1 = m_1\omega_B^2 \tag{6}$$

$$M = \frac{Nm_1}{2}\left[\left(\frac{\omega_{T1}^2+\omega_{T2}^2}{\omega_B^2} - \frac{\omega_{T1}^2\omega_{T2}^2}{\omega_B^4} - 1\right)^{-1} - 1\right] \tag{7}$$

$$k_x = \frac{Nm_1\omega_B^2}{2}\left[\left(\frac{\omega_{T1}^2+\omega_{T2}^2}{\omega_B^2} - 1\right)\left(\frac{\omega_{T1}^2+\omega_{T2}^2}{\omega_B^2} - \frac{\omega_{T1}^2\omega_{T2}^2}{\omega_B^4} - 1\right)^{-1} - 1\right] \tag{8}$$

Note that,

$$\omega_R = \omega_B\sqrt{\left(1+\frac{m_1NR^2}{J}\right)} \tag{9}$$

i.e. the 0-ND modal frequency is higher than the blade frequency.

DETERMINATION OF THE MOST RESPONSIVE BLADE

The displacement of a blade relative to the hub due to an order excitation is termed *the order response* which is proportional to the strain/stress in the blade. For a tuned wheel, the blades produce the same order response. This is not true for a mistuned wheel. There must be a blade experiencing *the maximum order response* of all the blades. As excitation frequency changes the maximum order response changes as well and may occur at a different blade. The maximum of the order responses of all the blades over all the excitation frequencies is termed *the peak maximum order response* (PMOR). It is important to determine which blade has the PMOR. If parameters of a mistuned wheel are completely known, a simple calculation can give the answer. Thus mistuning identification is practically important and will be dealt with below. An alternative is to use statistics. If a blade with a particular feature has a high probability (*e.g.* more than 90%) of having the PMOR and this feature can be easily identified, then the most responsive blade can be practically labelled. To do so, blades in a wheel must be numbered according to the blade feature. Blades from different wheels have the same number if the blades possess the same feature.

To number the blades of a mistuned wheel, measurement is performed for *the tip-to-tip frequency response function matrix,* denoted by $\widetilde{\mathbf{H}}(\omega)$, where, ω is the radian frequency. This is a $N \times N$ matrix and is constructed from the normal displacements of the blade tips observed from the ground due to a unit normal point force at the same or another blade tip. Responses of the blades, denoted by $\mathbf{q}^e(\omega)$ and calculated from

$$\widetilde{\mathbf{q}}^e(\omega) = (\widetilde{q}_1^e(\omega), \widetilde{q}_2^e(\omega), \cdots \widetilde{q}_N^e(\omega))^T = \widetilde{\mathbf{H}}(\omega)(e^{in\alpha_1}, e^{in\alpha_2}, \cdots e^{in\alpha_N})^T \tag{10}$$

are termed *the experimental order responses* of the blades subject to the *n*th order excitation. Due to the vibration of the hub, an experimental order response is in general different from the corresponding order response which is observed from the hub. The maximum of the experimental order response of a blade over a frequency range is then determined and compared to those of other blades. Blades are then numbered based on their maximum experimental order responses: the higher the maximum experimental order response is, the lower is the blade number.

Based on this blade numbering method and the lumped parameter model, calculations are carried out for a large number (3000) of mistuned wheels to produce the occurrences for a blade to have the PMOR. The corresponding tuned wheel is the one shown in Fig 1 and Table 1. A loss factor of 0.005 is estimated for material damping. Mistuning is described by random blade frequencies which follow a normal distribution with the mean being 6427 Hz and the standard deviation 170 Hz. The probability of a blade to have the PMOR is shown in Fig 2 for five (the 4^{th}, 5^{th}, 6^{th}, 7^{th} and 8^{th}) excitation orders. It can be seen that the No. 1 blade has more than 95% probability to have the PMOR. In other words, the blade having the peak maximum experimental order response almost certainly has the PMOR. It must be addressed that, the blade having the PMOR usually changes as the excitation order changes.

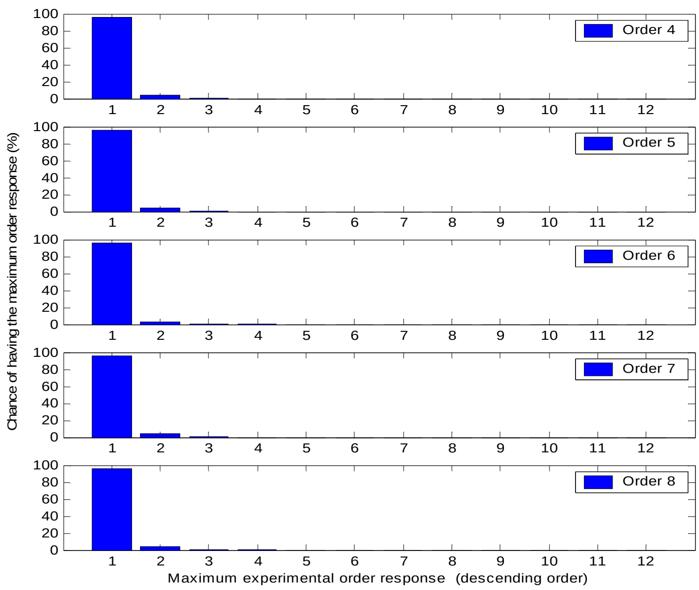

Figure 2 Probability of a blade to have the peak maximum order response

DISTRIBUTION OF THE PEAK MAXIMUM ORDER RESPONSE

Fig. 3 shows the PMOR of the 3000 wheel samples. To determine which distribution best fits the PMOR realisations, probability plots are produced using Minitab for a number of distributions. It is assumed that for any mistuned wheel, the frequency at which the PMOR occurs will be excited at a 100% chance. This indicates that statistics should be performed for the PMOR against mistuned wheel samples. It is found two distributions fit the data well: the 3-parameter lognormal distribution (Fig. 4 for the 4th order excitation and a factor of 1×10^{-6} has been dropped) and the 3-parameter Gamma distribution (not shown here). The 3-parameter Weibull distribution is not a good fit, though it has been suggested for aero engine turbofan in some publications [*e.g.* 8].

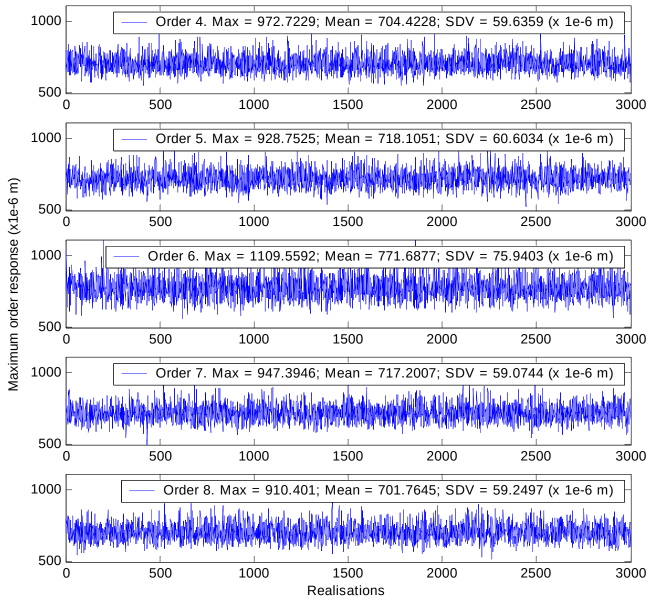

Figure 3 Peak maximum order responses of the wheel samples

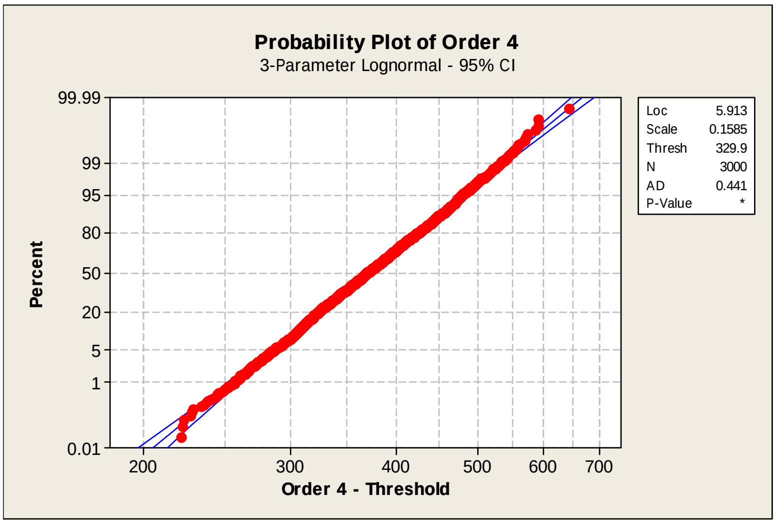

Figure 4 Probability plots for the peak maximum 4th order responses of the wheel samples: 3-parameter lognormal

MISTUNING IDENTIFICATION

The FE equation of motion of a mistuned bladed wheel may be written as

$$(\mathbf{M}+\Delta\mathbf{M})\ddot{\mathbf{q}}+(\mathbf{K}+\Delta\mathbf{K})\mathbf{q}=\tilde{\mathbf{Q}}e^{i\omega t} \tag{11}$$

where, matrices $\mathbf{M}$ and $\mathbf{K}$ represent the tuned mass and stiffness matrices while $\Delta\mathbf{M}$ and $\Delta\mathbf{K}$ denote mistuning in mass and stiffness. The order of the equation is reduced by expressing mistuned vibration in terms of a number of *N* tuned modes, *i.e.*

$$\mathbf{q} = [\boldsymbol{\varphi}_1\boldsymbol{\varphi}_2 \cdots \boldsymbol{\varphi}_N]\boldsymbol{\beta}e^{i\omega t} = \boldsymbol{\Phi}\boldsymbol{\beta}e^{i\omega t} \tag{12}$$

where, $\boldsymbol{\Phi} = [\boldsymbol{\varphi}_1\boldsymbol{\varphi}_2 \cdots \boldsymbol{\varphi}_N]$ is a matrix formed by the tuned modes and $\boldsymbol{\beta}$ is the weight vector. An assumption has been made here that the mistuned vibration is still within the sub-space spanned by these tuned modes. Substituting Eq. (12) into (11) and pre-multiplying $\boldsymbol{\Phi}^H$, yields

$$-\omega^2(\mathbf{M}^* + \boldsymbol{\Phi}^H \Delta\mathbf{M}\boldsymbol{\Phi})\boldsymbol{\beta} + (\mathbf{K}^* + \boldsymbol{\Phi}^H \Delta\mathbf{K}\boldsymbol{\Phi})\boldsymbol{\beta} = \boldsymbol{\Phi}^H \tilde{\mathbf{Q}} \tag{13}$$

where $\mathbf{M}^*$ and $\mathbf{K}^*$ are diagonal matrices formed by the modal mass and stiffness of the tuned system. If mass and stiffness matrices mistuning (*i.e.* $\boldsymbol{\Phi}^H \Delta\mathbf{M}\boldsymbol{\Phi}$ and $\boldsymbol{\Phi}^H \Delta\mathbf{K}\boldsymbol{\Phi}$) is known, then forced vibration can be determined by solving this equation.

To identify mistuning, use is made of the tip-to-tip frequency response matrix, $\tilde{\mathbf{H}}(\omega)$, defined above. Define the force vector of an order excitation:

$$\mathbf{F}(t) = (\tilde{F}_1, \tilde{F}_2, \cdots \tilde{F}_N)^T e^{i\omega t} = \tilde{\mathbf{F}}e^{i\omega t} \tag{14}$$

in which the forces are applied at the blade tips and normal to the blade surfaces. The global force vector, $\tilde{\mathbf{Q}}$, in Eq. (13) can be generated accordingly. The normal displacement amplitudes of the tips due to this order excitation can be calculated using

$$\tilde{\mathbf{q}}^e = \tilde{\mathbf{H}}\tilde{\mathbf{F}} \tag{15}$$

where, $\tilde{\mathbf{q}}^e = (\tilde{q}_1^e, \tilde{q}_2^e, \ldots \tilde{q}_N^e)^T$ is the vector of the normal tip displacement amplitudes.

According to Eq. (12), the tip displacement vector, $(u_s, v_s, w_s)^T$ of the *s*th blade, is given by

$$(u_s, v_s, w_s)^T = \sum_{m=1}^{N} \beta_m (\varphi_{1m}^{(s)}, \varphi_{2m}^{(s)}, \varphi_{3m}^{(s)})^T \tag{16}$$

where, $\varphi_{1m}^{(s)}, \varphi_{2m}^{(s)}$ and $\varphi_{3m}^{(s)}$ are the *x*-, *y*- and *z*-components of the tip displacement of the s^{th} blade in the *m*th tuned mode. If the directional cosines vector of the tip normal is denoted by $\tilde{\mathbf{a}}_s$, then from Eq. (16)

$$\tilde{\mathbf{a}}_s^T (u_s, v_s, w_s)^T = \sum_{m=1}^{N} \beta_m \tilde{\mathbf{a}}_s^T (\varphi_{1m}^{(s)}, \varphi_{2m}^{(s)}, \varphi_{3m}^{(s)})^T \tag{17}$$

In Eq. (17), the term on the left hand side is $\tilde{q}_s^e$. Denoting

$$a_{sm} = \tilde{\mathbf{a}}_s^T (\varphi_{1m}^{(s)}, \varphi_{2m}^{(s)}, \varphi_{3m}^{(s)})^T \tag{18}$$

then Eq. (17) becomes

$$\sum_{m=1}^{N} a_{sm}\beta_m = \tilde{q}_s^e, \text{ or } \mathbf{A}\boldsymbol{\beta} = \tilde{\mathbf{q}}^e \tag{19}$$

from which $\boldsymbol{\beta}$ can be virtually expressed as

$$\boldsymbol{\beta} = \mathbf{A}^{-1}\tilde{\mathbf{q}}^e = \mathbf{A}^{-1}\tilde{\mathbf{H}}\tilde{\mathbf{F}} \tag{20}$$

Using Eq. (20), $\boldsymbol{\beta}$ can be calculated for different excitation frequencies and orders. Two excitation frequencies, ω_1 and ω_2, are chosen so that $\tilde{\mathbf{H}}(\omega_1)$ and $\tilde{\mathbf{H}}(\omega_2)$ are regular matrices. Let

$$\tilde{\mathbf{F}}_j = (e^{ir_j\alpha_1}, e^{ir_j\alpha_2}, \cdots e^{ir_j\alpha_N})^T \tag{21}$$

where, $j = 1, 2, \cdots N$ and r_j is a number which may or may not be an integer. The orders, r_j, should be chosen in such a way that the matrix $[\tilde{\mathbf{F}}_1, \tilde{\mathbf{F}}_2, \cdots \tilde{\mathbf{F}}_N]$ is regular. The corresponding global force vector is denoted by $\tilde{\mathbf{Q}}_j(\omega_1)$ for the first excitation frequency and $\tilde{\mathbf{Q}}_j(\omega_2)$ for the second. Two $N \times N$ matrices thus can be formed

$$\mathbf{B}_1 = \mathbf{A}^{-1}\tilde{\mathbf{H}}(\omega_1)[\tilde{\mathbf{F}}_1, \tilde{\mathbf{F}}_2, \cdots \tilde{\mathbf{F}}_N],\ \mathbf{B}_2 = \mathbf{A}^{-1}\tilde{\mathbf{H}}(\omega_2)[\tilde{\mathbf{F}}_1, \tilde{\mathbf{F}}_2, \cdots \tilde{\mathbf{F}}_N] \tag{22}$$

They are regular matrices. Inserting Eq. (22) into (13) yields equations from which $\mathbf{\Phi}^H \Delta\mathbf{M}\mathbf{\Phi}$ and $\mathbf{\Phi}^H \Delta\mathbf{K}\mathbf{\Phi}$ can be determined

$$\mathbf{\Phi}^H \Delta\mathbf{M}\mathbf{\Phi} = -\mathbf{M}^* + \frac{\mathbf{\Phi}^H}{\omega_2^2 - \omega_1^2}\left\{[\tilde{\mathbf{Q}}_1(\omega_1)\cdots\tilde{\mathbf{Q}}_N(\omega_1)]\mathbf{B}_1^{-1} - [\tilde{\mathbf{Q}}_1(\omega_2)\cdots\tilde{\mathbf{Q}}_N(\omega_2)]\mathbf{B}_2^{-1}\right\} \tag{23a}$$

$$\mathbf{\Phi}^H \Delta\mathbf{K}\mathbf{\Phi} = -\mathbf{K}^* + \frac{\mathbf{\Phi}^H}{\omega_2^2 - \omega_1^2}\left\{\omega_2^2[\tilde{\mathbf{Q}}_1(\omega_1)\cdots\tilde{\mathbf{Q}}_N(\omega_1)]\mathbf{B}_1^{-1} - \omega_1^2[\tilde{\mathbf{Q}}_1(\omega_2)\cdots\tilde{\mathbf{Q}}_N(\omega_2)]\mathbf{B}_2^{-1}\right\} \tag{23b}$$

Now Eq. (13) can be used to predict order responses of the blades in a mistuned wheel. Example calculations (not presented here due to page limit) show that the mistuning identification method is able to produce accurate order response predictions for frequencies around and below the blade frequencies.

CONCLUSION

This paper presents research performed at Holset into the dynamics of mistuned radial turbine wheels. Based on FE analysis, a simple lumped parameter model is developed for mistuned turbine wheels. Using this model, it is shown that the blade having the peak maximum experimental order response will at a probability of more than 95% have the peak maximum order response, thus the most responsive blade in a given wheel can be practically identified for stain gauging. Peak maximum order responses of mistuned turbine wheels are found to follow the 3-parameter lognormal distribution or 3-parameter Gamma distribution, rather than the Weibull distribution. A mistuning identification method is also proposed based on the tip-to-tip frequency response function matrix and this method is shown to produce accurate order response predictions.

It should be pointed out that the effect of wheel rotation and temperature has not yet been considered. This must be one of the topics of further work since turbocharger rotors run at very high speeds and the turbine wheels are driven by high temperature gases. Further work will also be directed to other aspects: for example, the mechanism making a tuned wheel so sensitive to small mistuning, designs of intentional mistuning and explanation of the veer phenomenon, etc.

REFERENCES

1 C S Manohar and R A Ibrahim, ‘Progress in structural dynamics with stochastic parameter variations: 1987 to 1998’, *Applied Mechanics Review*, 1999 **52** 177-197.

2 S Adhiakri and M I Friswell, ‘Random eigenvalue problems in structural dynamics’, 45th AIAA/ASME/ASCE/AHS/ASC Conf *Structures, Structural Dynamics & Materials*, Palm Springs, California, USA, April 2004.

3 D J Ewins, ‘The effect of detuning upon the forced vibration of bladed disks’, *Journal of Sound and Vibration*, 1969 **9** 65-79.

4 J H Griffin and T M Hoosac, 'Model development and statistical investigation of turbine blade mistuning', *ASME Journal of Vibration, Acoustics, Stress and Reliability Design*, 1984 **106** 204-210.

5 A V Srinivasan, 'Flutter and resonant vibration characteristics of engine blades', *ASME Journal of Engineering for Gas Turbine and Power*, 1997 **119** 742-775.

6 R Bladh, M P Castanier and C Pierre, 'Component-mode-based reduced order modelling techniques for mistuned bladed disks—Part I: Theoretical models', *ASME Journal of Engineering for Gas Turbine and Power*, 2001 **123** 89-99.

7 R Bladh, M P Castanier and C Pierre, 'Component-mode-based reduced order modelling techniques for mistuned bladed disks—Part II: Application', *ASME Journal of Engineering for Gas Turbine and Power*, 2001 **123** 100-108.

8 R Bladh, C Pierre, M P Castanier and M J Kruse, 'Dynamic response predictions for a mistuned industrial turbomachinery rotor using reduced-order modelling', *ASME Journal of Engineering for Gas Turbine and Power*, 2002 **124** 311-324.

9 F Moyroud, T Fransson and G Jacquet-Richardet, 'A comparison of two finite element reduction techniques for mistuned bladed disks', *ASME Journal of Engineering for Gas Turbine and Power*, 2002 **124** 942-952.

10 E P Petrov, K Y Sanliturk and D J Ewins, 'A new method for dynamic analysis of mistuned bladed disks based on the exact relationship between tuned and mistuned systems', *ASME Journal of Engineering for Gas Turbine and Power*, 2002 **124** 586-597.

11 D M Feiner and J H Griffin, 'A fundamental model of mistuning for a single family of modes', *ASME Journal of Turbomachinery*, 2002 **124** 597-605.

12 A J Rivas-Guerra, M P Mignolet and J P Delor, 'Identification of mistuning characteristics of bladed disks from free response data—Part I', *ASME Journal of Engineering for Gas Turbine and Power*, 2001 **123** 395-403.

13 A J Rivas-Guerra, M P Mignolet and J P Delor, 'Identification of mistuning characteristics of bladed disks from free response data—Part II', *ASME Journal of Engineering for Gas Turbine and Power*, 2001 **123** 404-411.

14 D M Feiner and J H Griffin, 'Mistuning identification of bladed disks using a fundamental mistuning model—Part I: Theory', *ASME Journal of Turbomachinery*, 2004 **126** 150-158.

15 D M Feiner and J H Griffin, 'Mistuning identification of bladed disks using a fundamental mistuning model—Part II: Application', *ASME Journal of Turbomachinery*, 2004 **126** 159-165.

16 O O Bendiksen, 'Localisation phenomena in structural dynamics', *Chaos, Solitons and Fractals*, 2000 **11** 1621-1660.

17 M P Castanier and C Pierre, 'Using Intentional Mistuning in the Design of Turbomachinery Rotors', *AIAA Journal*, 2002 **40** 2077-2086.

18 M S Shahruz, 'Elimination of vibration localisation in mistuned periodic structures', *Journal of Sound and Vibration*, 2005 **281** 452-462.

19 D L Thomas, 'Dynamics of rotationally periodic structures', *International Journal of Numerical Methods in Engineering*, 1979 **14** 81-102.